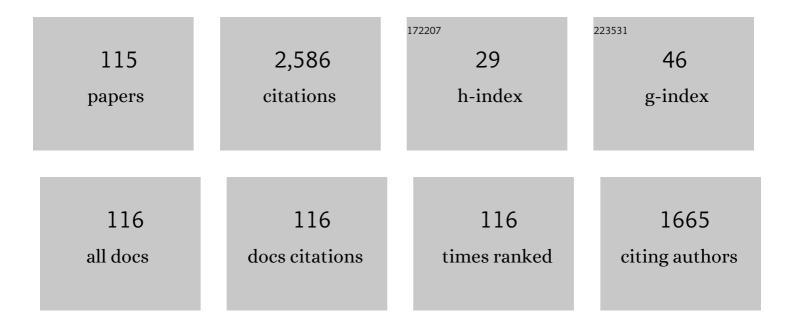
List of Publications by Year in descending order

Source: https://exaly.com/author-pdf/8766814/publications.pdf Version: 2024-02-01



#	Article	IF	CITATIONS
1	Selectively buried growth of heavily B doped diamond layers with step-free surfaces in N doped diamond (111) by homoepitaxial lateral growth. Applied Surface Science, 2022, , 153340.	3.1	1
2	Impact of nitrogen doping on homoepitaxial diamond (111) growth. Diamond and Related Materials, 2022, 125, 108997.	1.8	0
3	ãf€ã,¤f¤f¢ãf³ãf‰é«~哿³¢ãf»ãf'ãf-ãf¼ãf‡ãfã,¤,¹å¿œç"¨ã«å'ã'ã¥é‡'属â€é…,化膜â€åŠå°Žä½"ï¼^MO	Sï¹ <b>⁄@‰</b> 界	Ĩé¢ã®ç¾çÇ <mark>¶</mark>
4	Inversion channel MOSFET on heteroepitaxially grown free-standing diamond. Carbon, 2021, 175, 615-619.	5.4	9
5	Mechanical damage-free surface planarization of single-crystal diamond based on carbon solid solution into nickel. Diamond and Related Materials, 2021, 116, 108390.	1.8	1
6	Inversion-type p-channel diamond MOSFET issues. Journal of Materials Research, 2021, 36, 4688-4702.	1.2	13
7	Insight into temperature impact of Ta filaments on high-growth-rate diamond (100) films by hot-filament chemical vapor deposition. Diamond and Related Materials, 2021, 118, 108515.	1.8	8
8	Fabrication of inversion p-channel MOSFET with a nitrogen-doped diamond body. Applied Physics Letters, 2021, 119, .	1.5	11
9	Energy distribution of Al2O3/diamond interface states characterized by high temperature capacitance-voltage method. Carbon, 2020, 168, 659-664.	5.4	20
10	Insight into Al2O3/B-doped diamond interface states with high-temperature conductance method. Applied Physics Letters, 2020, 117, .	1.5	11
11	Formation of U-shaped diamond trenches with vertical {111} sidewalls by anisotropic etching of diamond (110) surfaces. Diamond and Related Materials, 2020, 103, 107713.	1.8	15
12	Temperature dependence of diamond MOSFET transport properties. Japanese Journal of Applied Physics, 2020, 59, SGGD19.	0.8	4
13	Step-edge growth and doping of diamond. Semiconductors and Semimetals, 2020, 103, 57-72.	0.4	1
14	Highâ€Rate Growth of Single rystalline Diamond (100) Films by Hotâ€Filament Chemical Vapor Deposition with Tantalum Filaments at 3000 °C. Physica Status Solidi (A) Applications and Materials Science, 2019, 216, 1900244.	0.8	7
15	Inversion channel mobility and interface state density of diamond MOSFET using N-type body with various phosphorus concentrations. Applied Physics Letters, 2019, 114, .	1.5	19
16	Conductive-probe atomic force microscopy and Kelvin-probe force microscopy characterization of OH-terminated diamond (111) surfaces with step-terrace structures. Japanese Journal of Applied Physics, 2019, 58, SIIB08.	0.8	5
17	Homoepitaxial Diamond Growth by Plasma-Enhanced Chemical Vapor Deposition. Topics in Applied Physics, 2019, , 1-29.	0.4	3
18	Highâ€Rate Growth of Singleâ€Crystalline Diamond (100) Films by Hotâ€Filament Chemical Vapor Deposition with Tantalum Filaments at 3000 °C. Physica Status Solidi (A) Applications and Materials Science, 2019, 216–1970071	0.8	1

#	Article	IF	CITATIONS
19	Anisotropic diamond etching through thermochemical reaction between Ni and diamond in high-temperature water vapour. Scientific Reports, 2018, 8, 6687.	1.6	41
20	Direct observation of inversion capacitance in p-type diamond MOS capacitors with an electron injection layer. Japanese Journal of Applied Physics, 2018, 57, 04FR01.	0.8	14
21	Formation of atomically flat hydroxyl-terminated diamond (1â€ <sup>−</sup> 1â€ <sup>−</sup> 1) surfaces via water vapor annealing. Applied Surface Science, 2018, 458, 222-225.	3.1	23
22	Quantitative relevance of substitutional impurities to carrier dynamics in diamond. Physical Review Materials, 2018, 2, .	0.9	9
23	Fabrication of graphene on atomically flat diamond (111) surfaces using nickel as a catalyst. Diamond and Related Materials, 2017, 75, 105-109.	1.8	22
24	Self-separation of freestanding diamond films using graphite interlayers precipitated from C-dissolved Ni substrates. Journal of Crystal Growth, 2017, 470, 104-107.	0.7	6
25	Mechanism of anisotropic etching on diamond (111) surfaces by a hydrogen plasma treatment. Applied Surface Science, 2017, 422, 452-455.	3.1	22
26	Diamond Schottky-pn diode using lightly nitrogen-doped layer. Diamond and Related Materials, 2017, 75, 152-154.	1.8	37
27	B-doped diamond field-effect transistor with ferroelectric vinylidene fluoride–trifluoroethylene gate insulator. Japanese Journal of Applied Physics, 2017, 56, 10PF06.	0.8	3
28	Influence of substrate misorientation on the surface morphology of homoepitaxial diamond (111) films. Physica Status Solidi (A) Applications and Materials Science, 2016, 213, 2051-2055.	0.8	10
29	H-terminated diamond field effect transistor with ferroelectric gate insulator. Applied Physics Letters, 2016, 108, 242101.	1.5	7
30	Inversion channel diamond metal-oxide-semiconductor field-effect transistor with normally off characteristics. Scientific Reports, 2016, 6, 31585.	1.6	150
31	Atomically flat diamond (100) surface formation by anisotropic etching of solid-solution reaction of carbon into nickel. Diamond and Related Materials, 2016, 68, 127-130.	1.8	20
32	Time-resolved cyclotron resonance on dislocation-free HPHT diamond. Diamond and Related Materials, 2016, 63, 38-42.	1.8	24
33	Homoepitaxial Diamond Growth by Plasma-Enhanced Chemical Vapor Deposition. Topics in Applied Physics, 2015, , 1-29.	0.4	9
34	Realization of Atomically Controlled Diamond Surfaces. Journal of the Japan Society for Precision Engineering, 2014, 80, 433-438.	0.0	0
35	Atomistic mechanism of perfect alignment of nitrogen-vacancy centers in diamond. Applied Physics Letters, 2014, 105, .	1.5	39
36	Density functional studies of surface potentials for hydrogen and oxygen atoms on diamond (111) surfaces. Japanese Journal of Applied Physics, 2014, 53, 02BD01.	0.8	3

#	Article	IF	CITATIONS
37	Anisotropic lateral growth of homoepitaxial diamond (111) films by plasma-enhanced chemical vapor deposition. Japanese Journal of Applied Physics, 2014, 53, 04EH04.	0.8	19
38	Free exciton luminescence from a diamond p–i–n diode grown on a substrate produced by heteroepitaxy. Physica Status Solidi (A) Applications and Materials Science, 2014, 211, 2251-2256.	0.8	14
39	Perfect selective alignment of nitrogen-vacancy centers in diamond. Applied Physics Express, 2014, 7, 055201.	1.1	84
40	Reduction of nâ€ŧype diamond contact resistance by graphite electrode. Physica Status Solidi - Rapid Research Letters, 2014, 8, 137-140.	1.2	16
41	Formation of Graphene-on-Diamond Structure by Graphitization of Atomically Flat Diamond (111) Surface. Japanese Journal of Applied Physics, 2013, 52, 110121.	0.8	37
42	Fabrication of (Bi,Pr)(Fe,Mn)O\$_{3}\$ Thin Films on Polycrystalline Diamond Substrates by Chemical Solution Deposition and Their Properties. Japanese Journal of Applied Physics, 2012, 51, 09LA08.	0.8	5
43	Isotope Effect of Deuterium Microwave Plasmas on the Formation of Atomically Flat (111) Diamond Surfaces. Japanese Journal of Applied Physics, 2012, 51, 090106.	0.8	4
44	Formation of Step-Free Surfaces on Diamond (111) Mesas by Homoepitaxial Lateral Growth. Japanese Journal of Applied Physics, 2012, 51, 090107.	0.8	19
45	Fractional Surface Termination of Diamond by Electrochemical Oxidation. Langmuir, 2012, 28, 47-50.	1.6	38
46	Isotope Effect of Deuterium Microwave Plasmas on the Formation of Atomically Flat (111) Diamond Surfaces. Japanese Journal of Applied Physics, 2012, 51, 090106.	0.8	2
47	Formation of Step-Free Surfaces on Diamond (111) Mesas by Homoepitaxial Lateral Growth. Japanese Journal of Applied Physics, 2012, 51, 090107.	0.8	19
48	Fabrication of (Bi,Pr)(Fe,Mn)O3Thin Films on Polycrystalline Diamond Substrates by Chemical Solution Deposition and Their Properties. Japanese Journal of Applied Physics, 2012, 51, 09LA08.	0.8	1
49	Electron emission from CVD diamond p–i–n junctions with negative electron affinity during room temperature operation. Diamond and Related Materials, 2011, 20, 917-921.	1.8	10
50	Effects of high-temperature annealing on electron spin resonance in SiOx films prepared by R. F. sputtering system. Journal of Non-Crystalline Solids, 2011, 357, 981-985.	1.5	11
51	The creation of a biomimetic interface between boron-doped diamond and immobilized proteins. Biomaterials, 2011, 32, 7325-7332.	5.7	31
52	Carrier transport of diamond p <sup>+</sup> â€iâ€n <sup>+</sup> junction diode fabricated using lowâ€resistance hopping p <sup>+</sup> and n <sup>+</sup> layers. Physica Status Solidi (A) Applications and Materials Science, 2011, 208, 937-942.	0.8	5
53	Annealing Effects on Cathodoluminescence Properties of SiOxFilms Deposited by Radio Frequency Sputtering. Japanese Journal of Applied Physics, 2011, 50, 01BF04.	0.8	1
54	Structure and Electrical Properties of (Pr, Mn)-Codoped BiFeO3â^•B-Doped Diamond Layered Structure. Electrochemical and Solid-State Letters, 2011, 14, G31.	2.2	6

#	Article	IF	CITATIONS
55	Improvement of (001)-oriented diamond p-i-n diode by use of selective grown n+ layer. Physica Status Solidi (A) Applications and Materials Science, 2010, 207, 2099-2104.	0.8	12
56	Diamond Schottkyâ€pn diode without tradeâ€off relationship between onâ€resistance and blocking voltage. Physica Status Solidi (A) Applications and Materials Science, 2010, 207, 2105-2109.	0.8	34
57	Electron Emission from a Diamond (111) p–i–n+Junction Diode with Negative Electron Affinity during Room Temperature Operation. Applied Physics Express, 2010, 3, 041301.	1.1	24
58	Growth of atomically step-free surface on diamond {111} mesas. Diamond and Related Materials, 2010, 19, 288-290.	1.8	33
59	Electron Emission from Diamond (111) p+-i-n+ Junction Diode. Materials Research Society Symposia Proceedings, 2009, 1203, 1.	0.1	0
60	Vertically aligned diamond nanowires: Fabrication, characterization, and application for DNA sensing. Physica Status Solidi (A) Applications and Materials Science, 2009, 206, 2048-2056.	0.8	48
61	Diamond Schottky p–n diode with high forward current density. Physica Status Solidi (A) Applications and Materials Science, 2009, 206, 2086-2090.	0.8	20
62	Dopingâ€induced changes in the valence band edge structure of homoepitaxial Bâ€doped diamond films below Mott's critical density. Physica Status Solidi (A) Applications and Materials Science, 2009, 206, 1991-1995.	0.8	5
63	Diamond Schottky-pn diode with high forward current density and fast switching operation. Applied Physics Letters, 2009, 94, .	1.5	77
64	Flattening of oxidized diamond (111) surfaces with H2SO4/H2O2 solutions. Diamond and Related Materials, 2009, 18, 213-215.	1.8	12
65	Selective Growth of Buried n+Diamond on (001) Phosphorus-Doped n-Type Diamond Film. Applied Physics Express, 2009, 2, 055502.	1.1	55
66	Electrical and light-emitting properties from (111)-oriented homoepitaxial diamond p–i–n junctions. Diamond and Related Materials, 2009, 18, 764-767.	1.8	18
67	Diamond nano-wires, a new approach towards next generation electrochemical gene sensor platforms. Diamond and Related Materials, 2009, 18, 910-917.	1.8	82
68	Characterization of specific contact resistance on heavily phosphorus-doped diamond films. Diamond and Related Materials, 2009, 18, 782-785.	1.8	35
69	Recovery of negative electron affinity by annealing on (111) oxidized diamond surfaces. Diamond and Related Materials, 2009, 18, 206-209.	1.8	9
70	High performance of diamond p+-i-n+ junction diode fabricated using heavily doped p+ and n+ layers. Applied Physics Letters, 2009, 94, .	1.5	73
71	Electrical and lightâ€emitting properties of homoepitaxial diamond p–i–n junction. Physica Status Solidi (A) Applications and Materials Science, 2008, 205, 2200-2206.	0.8	29
72	Electrical activity of doped phosphorus atoms in (001) nâ€ŧype diamond. Physica Status Solidi (A) Applications and Materials Science, 2008, 205, 2195-2199.	0.8	29

#	Article	IF	CITATIONS
73	Fermi level pinning-free interface at metals/homoepitaxial diamond (111) films after oxidation treatments. Applied Physics Letters, 2008, 92, 112112.	1.5	14
74	Low specific contact resistance of heavily phosphorus-doped diamond film. Applied Physics Letters, 2008, 93, .	1.5	68
75	Photoelectron emission from heavily B-doped homoepitaxial diamond films. Diamond and Related Materials, 2008, 17, 813-816.	1.8	3
76	Atomically flat diamond (111) surface formation by homoepitaxial lateral growth. Diamond and Related Materials, 2008, 17, 1051-1054.	1.8	43
77	Roughening of atomically flat diamond (111) surfaces by a hot HNO3/H2SO4 solution. Diamond and Related Materials, 2008, 17, 486-488.	1.8	14
78	Mapping of extended defects in B-doped (001) homoepitaxial diamond films by electron-beam-induced current (EBIC) and cathodoluminescence (CL) combination technique. Diamond and Related Materials, 2008, 17, 489-493.	1.8	5
79	Exciton-derived Electron Emission from (001) Diamond <i>p</i> – <i>n</i> Junction Diodes with Negative Electron Affinity. Applied Physics Express, 2008, 1, 015004.	1.1	8
80	Diamond nanowires, a new approach towards next generation electrochemical gene sensor platforms. Nature Precedings, 2008, , .	0.1	0
81	Electrochemical-microscopy analysis of bio-functionalized diamond surfaces. Materials Research Society Symposia Proceedings, 2007, 1039, 1.	0.1	Ο
82	Hillock-Free Heavily Boron-Doped Homoepitaxial Diamond Films on Misoriented (001) Substrates. Japanese Journal of Applied Physics, 2007, 46, 1469-1470.	0.8	28
83	Cycle of two-step etching process using ICP for diamond MEMS applications. Diamond and Related Materials, 2007, 16, 996-999.	1.8	47
84	Surface roughening of diamond (001) films during homoepitaxial growth in heavy boron doping. Diamond and Related Materials, 2007, 16, 767-770.	1.8	37
85	Inhomogeneous DNA bonding to polycrystalline CVD diamond. Diamond and Related Materials, 2007, 16, 1648-1651.	1.8	13
86	Leakage current analysis of diamond Schottky barrier diode. Applied Physics Letters, 2007, 90, 073506.	1.5	121
87	Electrochemical Grafting of Boron-Doped Single-Crystalline Chemical Vapor Deposition Diamond with Nitrophenyl Molecules. Langmuir, 2007, 23, 3466-3472.	1.6	106
88	Electrical and light-emitting properties of (001)-oriented homoepitaxial diamond p–i–n junction. Diamond and Related Materials, 2007, 16, 1025-1028.	1.8	18
89	Surface electronic properties on boron doped (111) CVD homoepitaxial diamond films after oxidation treatments. Diamond and Related Materials, 2007, 16, 831-835.	1.8	6
90	The role of boron atoms in heavily boron-doped semiconducting homoepitaxial diamond growth — Study of surface morphology. Diamond and Related Materials, 2007, 16, 409-411.	1.8	11

#	Article	IF	CITATIONS
91	Diamond and biology. Journal of the Royal Society Interface, 2007, 4, 439-461.	1.5	134
92	Direct observation of two-dimensional growth at SiO2/Si(111) interface. Thin Solid Films, 2007, 515, 7892-7898.	0.8	16
93	Surface conductive layers on (111) diamonds after oxygen treatments. Diamond and Related Materials, 2006, 15, 692-697.	1.8	20
94	Characterization of leakage current on diamond Schottky barrier diodes using thermionic-field emission modeling. Diamond and Related Materials, 2006, 15, 1949-1953.	1.8	66
95	Photo- and electrochemical bonding of DNA to single crystalline CVD diamond. Physica Status Solidi (A) Applications and Materials Science, 2006, 203, 3245-3272.	0.8	45
96	Periodically arranged benzene-linker molecules on boron-doped single-crystalline diamond films for DNA sensing. Electrochemistry Communications, 2006, 8, 844-850.	2.3	49
97	Energetics of dopant atoms in subsurface positions of diamond semiconductor. Superlattices and Microstructures, 2006, 40, 574-579.	1.4	4
98	High-Efficiency Excitonic Emission with Deep-Ultraviolet Light from (001)-Oriented Diamondp-i-nJunction. Japanese Journal of Applied Physics, 2006, 45, L1042-L1044.	0.8	52
99	Diamond Surface Modifications with Diazonium Salt. Materials Research Society Symposia Proceedings, 2006, 956, 1.	0.1	Ο
100	Utilization of Si atomic steps for Cu nanowire fabrication. Science and Technology of Advanced Materials, 2005, 6, 667-670.	2.8	4
101	Selective Growth of Monoatomic Cu Rows at Step Edges on Si(111) Substrates in Ultralow-Dissolved-Oxygen Water. Japanese Journal of Applied Physics, 2005, 44, L613-L615.	0.8	11
102	Selective Growth of Ag Nanowires on Si(111) Surfaces by Electroless Deposition. Journal of Physical Chemistry B, 2005, 109, 12655-12657.	1.2	12
103	Local Dielectric Degradation of Cu-Contaminated SiO <sub>2</sub> Thin Films. Solid State Phenomena, 2004, 95-96, 641-646.	0.3	1
104	Nonuniformity in Ultrathin SiO2on Si(111) Characterized by Conductive Atomic Force Microscopy. Japanese Journal of Applied Physics, 2004, 43, 7861-7865.	0.8	25
105	Leakage Current Distribution and Dielectric Breakdown of Cu-Contaminated Thin SiO[sub 2]. Journal of the Electrochemical Society, 2004, 151, F81.	1.3	4
106	Fabrication of Cu nanowires along atomic step edge lines on Si(111) substrates. Applied Surface Science, 2004, 237, 529-532.	3.1	10
107	Effect of SiO2Fence on Atomic Step Flow in Chemical Etching of Si Surface. Japanese Journal of Applied Physics, 2003, 42, L561-L563.	0.8	9
108	Topography Change Due to Multilayer Oxidation at SiO2/Si(111) Interfaces. Japanese Journal of Applied Physics, 2003, 42, 1903-1906.	0.8	13

#	Article	IF	CITATIONS
109	Selective Growth of Cu Nanowires on Si(111) Substrates. Japanese Journal of Applied Physics, 2003, 42, L1210-L1212.	0.8	17
110	Leakage Current Distribution of Cu-Contaminated Thin SiO2. Japanese Journal of Applied Physics, 2003, 42, L160-L162.	0.8	11
111	Atomic Topography Change of SiO2/Si Interfaces during Thermal Oxidation. Japanese Journal of Applied Physics, 2002, 41, L505-L508.	0.8	7
112	Leakage current distribution in ultrathin oxide on silicon surface with step/terrace structures. Thin Solid Films, 2002, 414, 56-62.	0.8	4
113	SiO2Surface and SiO2/Si Interface Topography Change by Thermal Oxidation. Japanese Journal of Applied Physics, 2001, 40, 4763-4768.	0.8	18
114	Nanometer Scale Height Standard Using Atomically Controlled Diamond Surface. Applied Physics Express, 0, 2, 055001.	1.1	20
115	Microscopic Evaluation of Al <sub>2</sub> O <sub>3</sub> /p-Type Diamond (111) Interfaces Using Scanning Nonlinear Dielectric Microscopy. Materials Science Forum, 0, 1062, 298-303.	0.3	1